

Inhibition of Tumor Growth and Metastasis Establishment by Adenovirus-mediated Gene Transfer Delivery of the Antiangiogenic Factor 16K hPRL

Ngoc-Quynh-Nhu Nguyen¹, Anne Cornet¹, Silvia Blacher², Sébastien P Tabruyn¹, Jean-Michel Foidart², Agnès Noël², Joseph A Martial¹ and Ingrid Struman¹

¹GIGA-Research, Molecular Biology and Genetic Engineering Unit, University of Liège, Belgium; ²GIGA-Research, Tumor and Development Biology Unit, University of Liège, Belgium.

Abstract

Tumor metastases, the most fearsome aspect of cancer, are generally resistant to conventional therapies. Angiogenesis is a crucial aspect of tumor growth and metastatic dissemination. Antiangiogenic therapy, therefore, holds potential as an attractive strategy for inhibiting metastasis development. Human 16K PRL (16K hPRL), a potent inhibitor of angiogenesis, has been demonstrated to prevent tumor growth in two xenograft mouse models, but whether it also affects tumor metastasis is unknown. In this study we will investigate the ability of 16K hPRL to prevent the establishment of metastasis. We demonstrate that 16K hPRL administered via adenovirus-mediated gene transfer, inhibits tumor growth by 86% in a subcutaneous (SC) B16-F10 mouse melanoma model. Computer-assisted image analysis shows that 16K hPRL treatment results in a reduction of tumor-vessel length and width, leading to a 57% reduction of average vessel size. In a pre-established tumor model, moreover, 16K hPRL can significantly delay tumor development. Finally, for the first time, we provide evidence that 16K hPRL considerably reduces the establishment of B16-F10 metastasis in an experimental lung metastasis model. Both the number and size of metastases are reduced by 50% in 16K hPRL-treated mice. These results highlight a potential role for 16K hPRL in anticancer therapy for both primary tumors and metastases.

INTRODUCTION

Tumor metastasis is the most fearsome aspect of cancer, responsible for most cancer patient morbidity and mortality. Metastases are resistant to conventional therapies because of their biological heterogeneity and the influence of the organ environment. Therapeutic strategies for preventing metastasis have the potential to reduce cancer mortality.^{1,2}

Angiogenesis, *i.e.*, the formation of new blood vessels from pre-existing ones, is a key event in tumor growth.³ This process is also crucial for tumor metastasis, as blood vessels provide tumor cells with an efficient route for leaving the primary site *via* the bloodstream.⁴ Angiogenesis is a complex process regulated by both activators and inhibitors of endothelial cell apoptosis, proliferation, migration, and organization. Many proteins (including their growth factors, their receptors, extracellular matrix proteins, and matrix metalloproteinases), are involved in this process. Great efforts have been made to discover new antiangiogenic factors, and antiangiogenic therapy is now considered an important approach to treating cancer.^{3,5}

16K PRL, the 16-kd N-terminal fragment of prolactin, is among the most potent of the known negative regulators of angiogenesis. We have previously shown that 16K PRL is antiangiogenic in both *in vitro* and *in vivo* models.⁶⁻¹¹ Very recently, human 16K PRL (16K hPRL) was shown to mediate postpartum cardiomyopathy.¹² 16K hPRL, produced by human HCT116 colon cancer cells, markedly reduces their ability to form subcutaneous (SC) tumors in *Rag1*^{-/-} mice.¹³ Furthermore, Kim and collaborators have demonstrated that adenovirus-mediated 16K hPRL expression by prostate cancer cells leads to tumor growth inhibition.¹⁴ However, it is unknown whether 16K PRL has an impact on metastasis. More recently, we have shown that 16K hPRL inhibits retinal neovascularization in a mouse model, in a non-cancer angiogenesis-related disease: oxygen-induced retinopathy.¹⁵ This ability to prevent angiogenesis in both tumor and retinopathy mouse models has raised great interest, notably in the potential use of 16K hPRL as an anticancer agent.

The usefulness of recombinant antiangiogenic proteins in the clinical treatment of cancer appears limited, due to the short half-life of the potentially therapeutic proteins (requiring repeated injections within a short period of time), the high therapeutic dose required, toxicity due to production in microorganisms, and high production costs. Gene therapy with angiogenesis inhibitors seems more promising, as it does not require a high dose of DNA molecules for injection and provides a sustained level of therapeutic molecules.¹⁶ Antiangiogenic gene therapy with viral vectors has proved effective in the treatment of cancer in animal models, notably in the case of vectors transferring an angiostatin, endostatin, PF-4, or TIMP-2 gene.¹⁶⁻¹⁸

In the present study, we have used well-characterized mouse models of primary tumor development and metastasis establishment (based on the use of B16-F10 melanoma cells) to investigate the effect of 16K hPRL on these processes. We provide evidence that 16K hPRL, administered by adenovirus-mediated gene transfer, can alter vascular morphology in primary tumors and reduce their growth. We also show, for the first time, that 16K hPRL exerts a striking inhibitory effect on metastasis development.

RESULTS

The 16K-Ad adenovirus vector drives expression of 16K hPRL

To analyze the effect of 16K hPRL on tumor growth and metastasis, we used 16K-Ad, an adenovirus vector that mediates 16K hPRL gene transfer. Western blot analysis of 16K hPRL produced in a medium conditioned by COS cells infected with 16K-Ad, showed high levels of 16K hPRL isoforms. Three bands for 16K hPRL were observed on the Western blot, the major band migrating slightly more slowly than the recombinant 16K hPRL produced in *Escherichia coli* (Figure 1). As previously shown in ref. 15, we suggest that 16K hPRL was mainly produced in a glycosylated form.

Figure 1: *16K-Ad adenovirus vector can drive expression of human 16K PRL (16K hPRL).* Thirty microliters of conditioned medium from a culture of COS cells infected with 16K-Ad [multiplicity of infection (MOI): 200 plaque forming units (pfu)/cell] or Null-Ad (MOI: 200pfu/cell) was subjected to Western blot analysis with an anti-16K hPRL antiserum. Thirty nanograms of recombinant 16K hPRL produced in *Escherichia coli* was loaded as a control (16K).

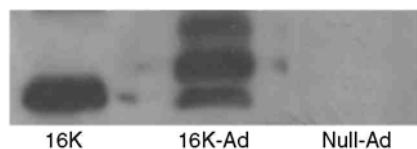
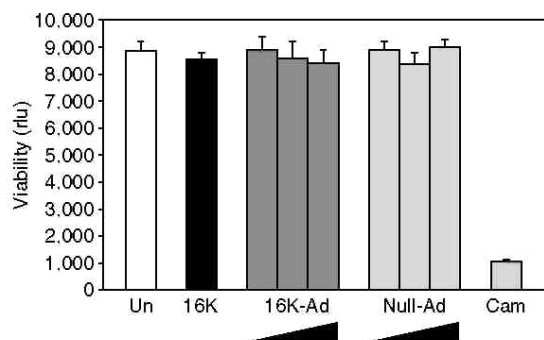


Figure 2: *Human 16K PRL (16K hPRL), 16K-Ad, and Null-Ad do not affect B16-F10 cell viability.* B16-F10 cell viability was unaffected when the cells were treated for 72 hours with recombinant 16K hPRL produced in *Escherichia coli* (50 nmol/l) or infected with either 16K-Ad [multiplicity of infection (MOI): 100, 200, and 400 plaque forming units (pfu)/cell] or Null-Ad (MOI: 100, 200, and 400pfu/cell). Un, untreated cells; Cam, camptothecin-treated cells, a positive control. Viability was evaluated by means of the calcein assay. rlu: relative luminescence unit. Each bar represents a mean \pm SEM, $n = 3$. Three different experiments were performed.



16K hPRL and the 16K-Ad adenovirus vector have no effect on B16-F10 viability

In order to determine whether recombinant 16K hPRL or adenovirus vector administration has a direct effect on B16-F10 tumor cells, cell viability was evaluated after incubating B16-F10 cells with 50nmol/l recombinant 16K hPRL produced in *E. coli*, or infecting them with 16K-Ad or Null-Ad at an increasing multiplicity of infection [100, 200, and 400 plaque forming units (pfu)/cell]. Results revealed no effect of recombinant 16K hPRL, 16K-Ad, or Null-Ad, whilst camptothecin, an inhibitor of topoi-somerase I used as a positive control, caused cell fluorescence to decrease dramatically (Figure 2).

Inhibition of tumor growth and modification of vascular morphology by 16K hPRL

To determine whether 16K hPRL affects B16-F10 melanoma tumor growth, we injected B16-F10 mouse melanoma cells SC into C57BL/6J mice and inoculated the mice with either 5×10^8 pfu of 16K-Ad or 5×10^8 pfu of Null-Ad control. Treatment with the adenovirus vector was repeated five times during the experiment. We monitored the effect of 16K hPRL on the tumor growth rate in two independent experiments. In both experiments, 16K hPRL-treated mice showed reduced tumor incidence and tumor growth (Figure 3a-c). At the end of the first experiment, the tumor incidence was 50% (5 of 10 tumors) in the 16K-Ad-treated mice and 100% (8 out of 8 tumors) in the control group. In a second experiment, the tumor incidence was 45% (5 of 11 tumors) in the 16K-Ad-treated mice and 89% (8 of 9 tumors) in the Null-Ad-treated mice (Figure 3a). On the day of kill, the mean tumor volume was 86% lower in the 16K hPRL group than in the control group (Figure 3b).

Considering the previously described ability of 16K hPRL to inhibit tumor angiogenesis *in vivo*,^{13,14} we evaluated the ability of 16K hPRL to affect tumor vascularization. Immunostaining for CD31 revealed interesting differences, in terms of morphology and size, between tumor vessels in the two groups: the blood vessels in 16K-Ad-treated tumors appeared smaller and collapsed (Figure 4a). Computer-assisted image analysis (Figure 4b, see Materials and Methods) was then used to quantify vessel density, vessel area density, and vessel size distribution. Surprisingly, the average vessel density (number of CD31-positive vessels/mm² tumor area) in Null-Ad-treated mice was 40% lower than in 16K-Ad-treated mice, whilst the percentage area covered by vessels was similar (Figure 4c and d). The difference between these two results can be explained as revealed by vessel size distribution histograms (Figure 4e): larger vessels disappear in the 16K-Ad-treated group, leading to a 57% reduction of average vessel size (Figure 4e and f).

Figure 3: Reduction of tumor growth by human 16K PRL. C57BL/6J mice were inoculated subcutaneously with 10^5 B16-F10 cells and, 1 day later, with 5×10^8 plaque forming units (pfu) of 16K-Ad or Null-Ad. Adenovirus vector injection was done five times. Two different experiments were performed. (a) Tumor incidence, defined as the percentage of mice bearing a tumor exceeding 100mm³ on the day of killing. (b) Mean tumor volume \pm SEM in mice implanted with 10^5 B16-F10 cells and treated every 2 days with 5×10^8 pfu 16K-Ad ($n = 10$) or control Null-Ad ($n = 8$) adenovirus vector. A significant difference with respect to the control (Null-Ad) is denoted by * $P < 0.05$. Two different experiments were performed, (c) Tumor volumes in mice at the end of the assay. Horizontal lines indicate the median tumor volume.

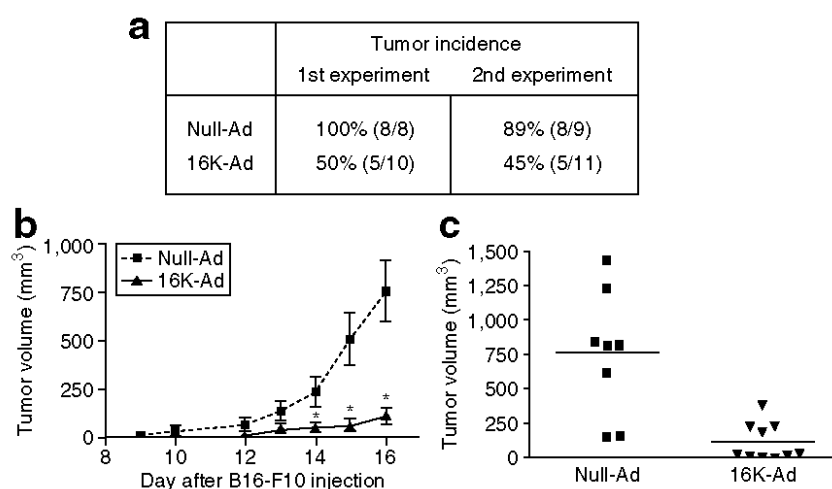


Figure 4: Reduction of tumor vessel area by human 16K PRL. (a) Representative photographs of tumor sections from 16K-Ad- and Null-Ad-inoculated mice, stained with anti-CD31 to reveal blood vessels (red) (x100 magnification). Bar: 100 μm . (b) Image processing as described under Materials and Methods. (A) Original red-green-blue color image. (B) Extraction of the red component. (C) Binary image of vessels (D) Labeled vessels. (c) The average vessel density + SEM was determined on CD31 -positive vessels in x100 power fields of each section as described under Materials and Methods. (d) Total vessel area + SEM was determined on CD31 -positive vessels in x100 power fields of each section as described under Materials and Methods. (e) The size distribution + SEM was determined on CD31 -positive vessels in x100 power fields of each section as described under Materials and Methods. (f) The average vessel size + SEM was determined on CD31-positive vessels in x100 power fields of each section as described under Materials and Methods. A significant difference with respect to the control (Null-Ad) is denoted by *, $P < 0.05$.

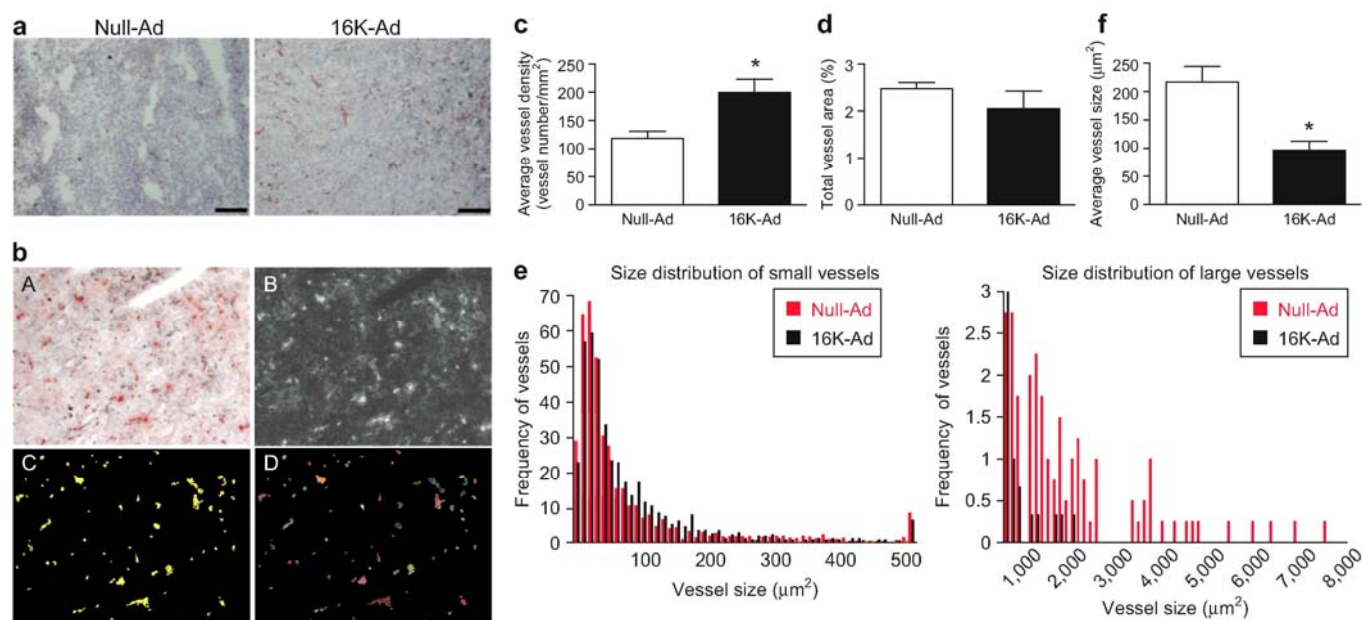
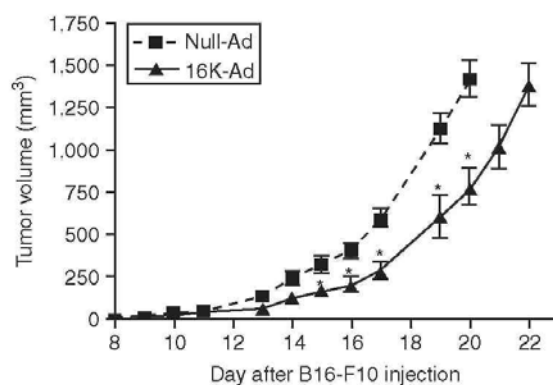


Figure 5: Human 16K PRL delays development of established tumors. C57BL/6J mice were inoculated subcutaneously with 10^5 B16-F10 cells. When their tumor size reached $\sim 50\text{mm}^3$, they were injected with 5×10^8 plaque forming units of 16K-Ad ($n = 6$) or control Null-Ad ($n = 8$) adenovirus vector. Mean tumor volume + SEM. A significant difference with respect to the control (Null-Ad) is denoted by *, $P < 0.05$.



These results show that the antiangiogenic factor 16K hPRL can strongly reduce the development of B16-F10 melanoma by altering tumoral vasculature.

To examine the effect of 16K hPRL on the growth of established tumors, we injected recombinant adenovirus into melanoma tumors in C57BL/6J mice. The tumors were established in mice by injection of B16-F10 into the flank, and the recombinant adenoviruses were injected later when the tumors reached $\sim 50\text{mm}^3$. SC injections of adenovirus vector were performed, 2 days apart. Significant inhibition of tumor growth was observed in 16K-Ad-treated mice: it took 2 days longer for tumors to reach the target size ($\sim 1.5\text{cm}^3$) (Figure 5) in these mice than in control mice.

Inhibition of experimental lung metastasis by 16K hPRL

Because metastasis is the leading cause of death in cancer patients, we then used an experimental lung metastasis assay to see whether 16K hPRL can affect metastatic outgrowth. The assay involved injecting B16-F10 cells into the tail vein of mice and observing the difference in metastasis establishment in the lung, between 16K-Ad-treated animals and untreated animals.

Western blot analysis revealed 16K hPRL in the sera of 16K-Ad-treated mice 7 and even 13 days after a single intravenous (IV) injection of adenovirus. 16K hPRL was not detected in the sera of Null-Ad-treated mice (Figure 6a). As previously observed *in vitro*, the predominant 16K hPRL isoform present in mouse serum migrated more slowly than recombinant 16K hPRL. Macroscopic observation of the lungs of mice treated with 10^9 pfu of 16K-Ad revealed only a few black tumor nodules, small in size. The lungs of control mice, on the other hand, showed multiple large tumor nodules that replaced the lung parenchyma (Figure 6b). Macroscopic quantification of tumor nodules on the lung surface revealed 50-60% fewer metastases in the 16K-Ad group than in the control group (Figure 6c). To further characterize the anti-metastatic effects of 16K hPRL, a histological examination of hematoxylin/eosin-stained lung tissues was done (Figure 6d). The extent of lung metastasis was assessed in terms of the number and size of metastases. Lungs of 16K-Ad-treated animals showed significantly fewer (50% fewer) metastases than those of control animals (Figure 6e). We graded the observed metastases according to three size levels: small (<200 μ m in diameter), medium (200 μ m to 1mm in diameter), and large (>1mm in diameter). The number of medium- and large-sized metastases was lower in the 16K-Ad-treated animals (Figure 6e).

We then repeated this experiment, repeating the injection and extending the period over which the effect of 16K hPRL was monitored. We first injected B6-F10 into the tail vein of each mouse. The mice then received two adenovirus vector injections, one after 2 days and one a week later. Thirteen days after the second 16K-Ad injection was made, we observed the striking effect that 16K hPRL had in preventing the establishment of metastases in the lung. The lungs of 16K-Ad-treated animals showed almost no tumor nodules, in contrast to control lungs. Yet 5 days later, the lungs of both groups looked similar, with tumor nodules covering the lung parenchyma (Figure 7a). Anti-CD31 was then used to immunostain blood vessels in sections of healthy lung and liver tissue from both 16K-Ad-treated, and untreated, mice. Treatment was found to have no significant effect on vascular morphology in either tissue (Figure 7b).

Taken together, these results show that 16K hPRL can inhibit tumor growth and metastasis establishment from B16-F10 melanoma *in vivo*.

Figure 6: Inhibition of experimental lung metastasis by human 16K PRL (16K hPRL). C57BL/6J mice were inoculated intravenously with 10^5 B16-F10 cells and, 2 days later, with 10^5 plaque forming units (pfu) of 16K-Ad or Null-Ad. Two different experiments were performed. (a) Western blot detection of 16K hPRL in 30 μ l immunoprecipitates from two mice inoculated with 16K-Ad (1-4) or Null-Ad (5-8). Odd number, immuno-precipitate from serum collected 7 days after adenoviral vector injection. Even number, immunoprecipitate from serum collected 13 days after adenoviral vector injection. (b) Representative photographs of lungs from mice treated with 16K-Ad or Null-Ad. (c) Mean number (\pm SEM) of metastatic foci on the surface of lungs from mice treated with 16K-Ad ($n = 9$) or Null-Ad ($n = 8$). (d) Representative lung sections stained with hematoxylin/eosin (x100 magnification). Bar: 100 μ m. (e) The number and size of internal pulmonary metastases were quantified. The histogram on the left represents the mean number of total metastases. The histogram on the right represents the distribution of metastases as a function of their diameter. Results are means \pm SEM for eight mice treated with 16K-Ad or five mice treated with Null-Ad. In c and e a significant difference with respect to the control (Null-Ad) is denoted by *, $P < 0.05$.

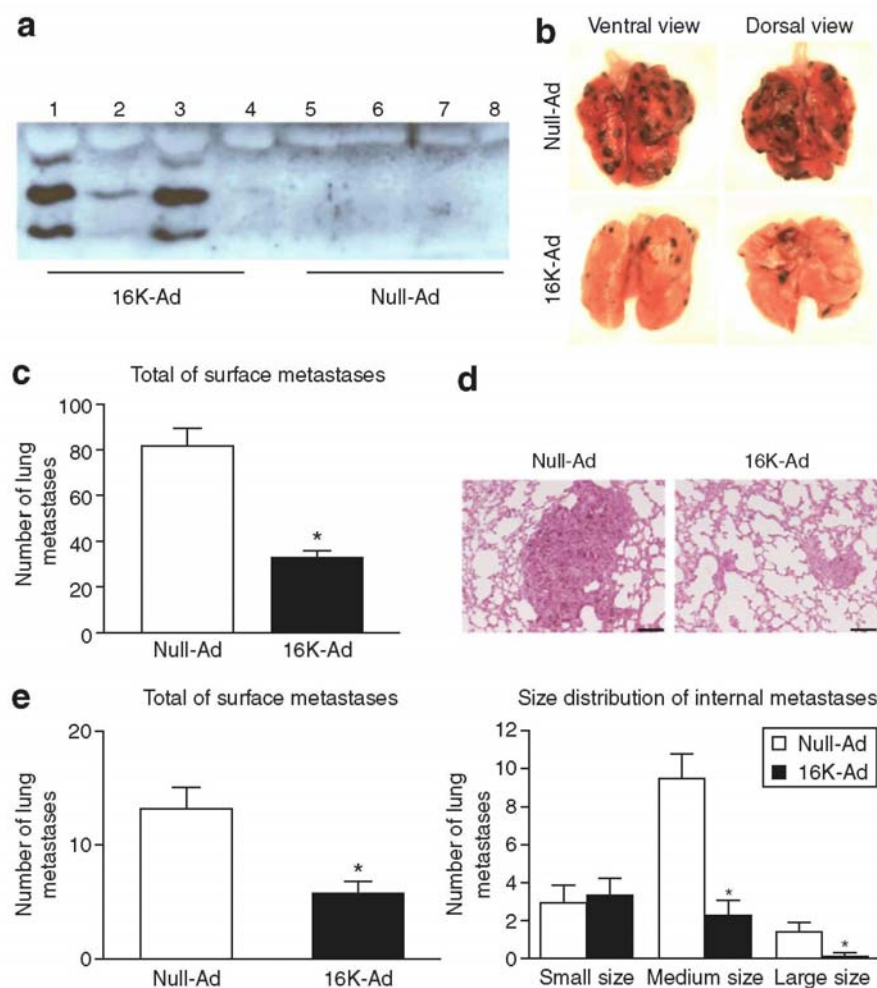
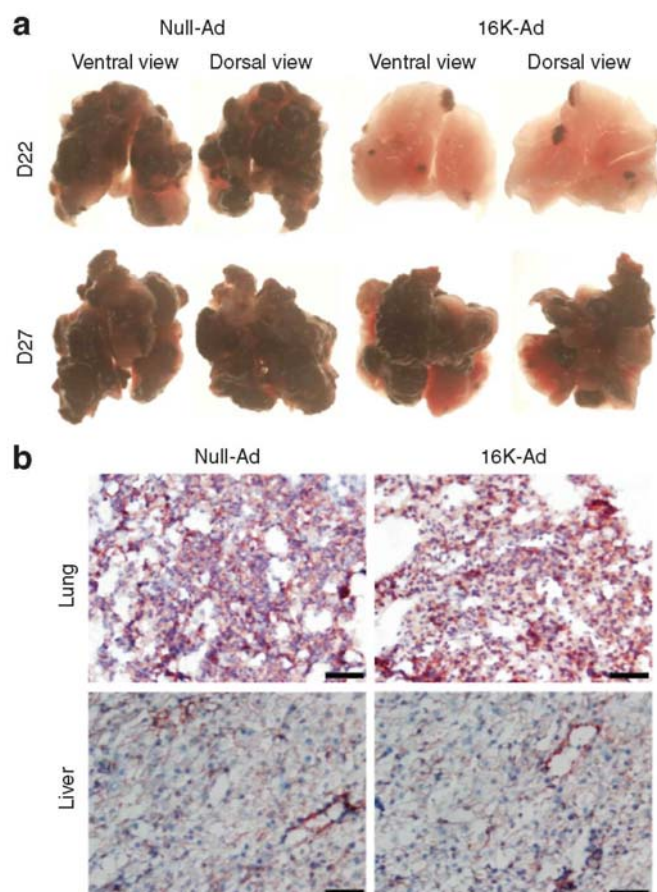


Figure 7: Metastasis establishment delayed by human 16K PRL.

(a) Representative photographs of lungs collected on days 22 and 27, from mice treated with 16K-Ad or Null-Ad. C57BL/6J mice were inoculated intravenously on day 0 with 10^5 B16-F10 cells and, 2 days later, with 10^9 plaque forming units (pfu) of 16K-Ad or Null-Ad. One week later, the mice were again inoculated with 10^9 pfu 16K-Ad or Null-Ad.
(b) Representative photographs of lung and liver sections from 16K-Ad- and Null-Ad inoculated mice (organs collected on day 22). The sections were stained with anti-CD31 to reveal blood vessels (red) (x200magnification). Bar: 100 μ m.



DISCUSSION

In the present study, we have evaluated the effects of 16K hPRL on two angiogenesis-dependent pathological phenomena: tumor growth and metastasis. B16-F10 murine melanoma cells were selected for their well-known high aggressiveness and their high lung metastatic potential.

We first showed that 16K hPRL gene therapy can effectively inhibit melanoma growth by 86% in a SC mouse model with tumor development. In a second experiment we showed, using a pre-established tumor model, that 16K hPRL can significantly delay tumor development, although the effect is weaker than observed in the previous model. The observed effect appears to be indirect, since neither recombinant 16K hPRL produced in *E. coli* nor the 16K-Ad adenovirus vector had any toxic effect on cultured B16-F10 cells. Prior to this work, only two reports have described the antitumor action of 16K hPRL: one by Bentzien *et al.*, who observed inhibition of tumor growth in *Rag1*^{-/-} mice treated with human HCT116 colon cancer cells expressing 16K hPRL,¹³ and one by Kim *et al.*, reporting tumor growth inhibition in *nu/nu* mice receiving implants of PC-3 or DU145 human prostate cancer cells expressing 16K hPRL.¹⁴ Both reports demonstrate a correlation between inhibition of *in vivo* tumor growth by 16K hPRL and decreased microvessel density in the tumor. These observations suggest that reduced blood vessel formation may contribute to decreased tumor growth after 16K PRL treatment. In our study, vessel density was not reduced, but for the first time, we provide evidence that 16K hPRL affects the morphology of tumor blood vessels. This idea has emerged from CD31 immunostaining and computerized quantification that reveal that blood vessels became smaller and somewhat collapsed after 16K hPRL treatment. Computer-assisted image analysis revealed a 57% decrease in average vessel size in Ad-16K-treated tumors as

compared to those treated by Null-Ad. Thrombospondin-2, another angiogenesis inhibitor, and cannabinoids^{19,20} are reported to similarly affect tumor-vessel morphology. In ref 19, the average vessel size was reduced in thrombospondin-2-overexpressing hA431 squamous tumors as compared to control tumors. In ref. 20, cannabinoids known to induce tumor regression in rodents were also shown to inhibit tumor angiogenesis. Although cannabinoid administration did not affect the microvascular count in gliomas, a notable effect was observed on blood vessel morphology: the vessels were characterized by very small and narrow capillaries.

How does 16K hPRL affect tumor vessel morphology? 16K hPRL might affect vascular tone. It is known to inhibit endothelial nitric oxide synthase activation by blocking intracellular Ca^{2+} mobilization, and this action results in inhibition of both angiogenesis and vasorelaxation.²¹

Tumor metastasis is the primary cause of mortality in cancer patients. Angiogenesis is important not only for primary tumor growth, but also for metastatic spread and growth of metastatic foci at distant sites. A high degree of tumor vascularization increases the likelihood that tumor cells will enter the bloodstream and metastasize.²² Thus, inhibition of angiogenesis is an attractive approach to limiting metastasis. Numerous anti-angiogenic factors, including angiostatin and endostatin, have been shown to inhibit both tumor development and metastatic spread and growth.^{23,24} To our knowledge, no previous report has described any inhibitory effect of 16K hPRL on metastasis. The metastatic process generally proceeds in steps, starting from the growth and vascularization of the primary tumor, escape of cells from the primary tumor into the bloodstream or lymph system (intravasation), transport of cells to distant organs, escape from the blood or lymph stream into the new tissue (extravasation), to growth and vascularization of the new metastatic tumor. The metastasis assay used here is designed to model the latter half of the metastatic process.¹ The results clearly show that 16K hPRL can exert a striking effect on lung metastasis development. Macroscopic and histological examinations revealed fewer and smaller metastases in the lungs of animals treated with the 16K-Ad adenovirus vector. Grading the observed metastases according to three sizes or levels further suggested that metastases are less invasive in 16K-Ad-treated mice than in control mice; this is because significantly fewer medium-sized (200 μ m to 1 mm in diameter) and large metastases (>1 mm in diameter) were observed in the former. This observation suggests that 16K affects both tumor cell implantation at a secondary site as well as tumor growth in this new environment. In accordance with this, a previous study has also shown that treatment with the angiogenesis inhibitor thienopyridine SR 25989 reduces the size and number of lung metastases in a similar metastasis model.²⁵ Our results show that it should be possible to limit the metastatic process to the development of small metastases that might mostly have only minimal clinical consequences for patients.

The inhibition of metastasis development in the lung correlates with the presence of 16K hPRL in serum samples from 16K-Ad-treated mice. The major 16K hPRL form detected in mouse serum appears to migrate more slowly than the 16K hPRL expressed in *E. coli*. This is in agreement with previous results suggesting that biologically active 16K hPRL exists in multiple forms arising most likely through post-translational modification.^{14,15} The major 16K hPRL isoform detected is probably the glycosylated form previously shown in a study by Pan.¹⁵ The relevance of such post-translational modifications is unknown.

In the metastasis model where the mice received two injections of 16K-Ad adenovirus vector, the efficacy of 16K hPRL administration was strong at first but then diminished, as attested by rapid development of tumor nodules in the lung. By day 27, treated and untreated lungs appeared equally affected, and this correlated with an undetectable serum level of 16K hPRL (data not shown), probably due to rapid clearance of the adenovirus vector by the murine organism. This result demonstrates the need to improve delivery of the vector to the tumor vasculature.

The major obstacle to achieving delivery of IV-administered adenoviral vectors to tumor-vasculature, endothelial cells and tumor cells is the nonspecific uptake of adenoviral vectors in the liver and other organs. To circumvent this problem, new adenovirus vectors targeting the tumor vasculature have been engineered. For example, Niu and collaborators have shown that introducing the RGD peptide into the adenoviral fiber protein increases binding of the adenoviral vector to tumor-vasculature endothelial cells and tumor cells.²⁶ Liu and collaborators, moreover, have shown that IV pre-administration of 6% hetastarch before adenoviral vector administration increases delivery of the adenoviral vector to tumor cells and their vasculature, reduces uptake by normal tissue, and reduces vector-mediated toxicity toward the liver.²⁷

In conclusion, this study demonstrates that 16K hPRL gene therapy can inhibit tumor growth. It is the first study to show inhibition of metastasis establishment by 16K hPRL treatment. These results suggest that the antiangiogenic factor 16K hPRL may have high therapeutic potential in cancer treatment. Further studies will be undertaken to determine whether 16K hPRL might also act on lymphangiogenesis, the formation of new lymph

vessels, to inhibit tumor and metastatic growth.

MATERIALS AND METHODS

Production of recombinant proteins

Recombinant 16K hPRL was produced in *E. coli* as previously described.¹⁰ The 16K hPRL coding sequence was obtained by site-directed mutagenesis performed on the complementary DNA encoding hPRL (minus the corresponding signal peptide) inserted into the pT7L expression vector.²⁸ An ATG was genetically engineered 5' from the first codon, Cys 58 (TGC) was mutated to serine (TCC) to avoid incorrect disulfite bonds, and Glu 140 (GAA) was mutated to TAA to generate a premature stop codon. Briefly, after induction of protein expression by treatment with isopropyl- β -D thiogalactopyranoside, the cells (*E. coli* BL21 DE3) were disrupted. The inclusion bodies were solubilized in 20mmol/l ethanalamine-HCl (pH 9) containing 8mol/l deionized urea and 1% β -mercaptoethanol, heated at 55 °C for 10 minutes, and incubated overnight at room temperature (RT). Denatured proteins were then purified as described in.¹⁰

The purity of the recombinant protein exceeded 95% (as estimated by Coomassie blue staining), and the endotoxin level was 0.0005 ng/ng recombinant protein, as quantified with the rapid endo test of the European Endotoxin Testing Service (BioWhittaker, Verviers, Belgium).

Adenovirus vectors

16K-Ad is a defective recombinant E1-E3-deleted adenovirus vector encoding a secreted peptide consisting of the first 139 amino acids of PRL. This adenovirus vector was constructed as described in ref. 15, using the Adeno-X expression system (BD Biosciences, Erembodegem, Belgium). Briefly, the 16K hPRL complementary DNA was cloned into a pShuttle vector in an expression cassette that was then inserted into the Adeno-X viral DNA. Recombinant adenoviruses were constructed and amplified in HEK 293 cells. The BD Adeno-X Virus Purification kit (BD Biosciences, Erembodegem, Belgium) and the Adeno-X Rapid Titer kit (BD Biosciences, Erembodegem, Belgium) were used to perform purification and titration, respectively, of the recombinant adenoviruses (by following the manufacturer's instructions). Null-Ad is a control adenovirus carrying an empty expression cassette.

Mice

Adult female C57BL/6J mice (6-8 weeks of age) purchased from the Central Animal Facility of Central Hospitalier Universitaire de Liège (Liège, Belgium) were used to assess tumor growth and experimental lung metastasis. The animal experiment protocols observed were all approved by the Institutional Ethics Committee of the University of Liège.

Cell cultures

COS cells were cultured in a low-glucose Dulbecco's modified Eagle's medium supplemented with 10% fetal calf serum and 4 mmol/l glutamine, 100U/ml penicillin, and 100 μ g/ml streptomycin at 37°C in a 5% CO₂ humid atmosphere. B16-F10 mouse melanoma cells were obtained from the American Type Culture Collection (CRL-6475, Rockville, MD) and cultured in a high-glucose Dulbecco's modified Eagle's medium supplemented with 10% fetal calf serum and 4mmol/l glutamine, 100U/ml penicillin, 100 μ g/ml streptomycin at 37°C in a 5% CO₂ humid atmosphere. All culture reagents were purchased from Invitrogen/Life Technologies (Paisley, Scotland).

Viability assay

B16-F10 cells were plated at a density of 2.5×10^4 cells/well (in 24-well plates) in 0.5 ml growth medium. Cells were infected with an adenovirus vector at an increasing multiplicity of infection or treated with 10 μ mol/l camptothecin (Sigma-Aldrich, Bornem, Belgium) for 72 hours. After washing with phosphate-buffered saline (PBS) and incubation with 1 μ mol/l calcein-AM (Calbiochem, San Diego, CA) for 30 minutes at RT, cell fluorescence was measured at 535 nm with a microplate reader (Wallac Victor²; Perkin Elmer, Norwalk, Finland).

***In vivo* tumorigenicity**

Subconfluent B16-F10 cells were trypsinized, washed, and resuspended in PBS. In the first experiment, cell suspension (10^5 cells in 50 μ l) was injected SC into the right flank of C57BL/6J mice. Groups of 12 mice were used and randomly divided. One day later, either a 5×10^8 pfu Null-Ad or 5×10^8 pfu 16K-Ad adenovirus vector, was inoculated SC into the peritumoral region. This injection was repeated every 3 days. Sixteen days after cell injection, the mice were killed and their tumors harvested. Tumor growth was assessed by measuring the length and width of each tumor, every 1 or 2 days, and calculating its volume by means of the formula: length \times width² \times 0.5 (ref. 29). Results are expressed as the mean tumor volume for each experimental group. Tumor incidence is defined as the percentage of mice bearing a tumor larger than 100 mm³ on the day of killing.

In a second experiment, when the tumors reached the average size of ~ 50 mm³, the mice were randomized and treated with either 5×10^8 pfu 16K-Ad or 5×10^8 pfu Null-Ad. Adenovirus administration was repeated every 2 days.

***In vivo* experimental lung metastasis assay**

In order to mimic the metastatic process, 10^5 B16-F10 cells in 50 μ l PBS were injected IV into the lateral tail vein of C57BL/6J mice. Groups of 12 mice were used and randomly divided. Two days later, 10^9 pfu Null-Ad or 16K-Ad adenovirus vector was injected IV into the lateral tail vein. Blood was collected 7 and 13 days after adenovirus vector injection. The mice were killed 15 days after tumor cell injection and their lungs harvested. Metastatic colonies were counted macroscopically on the lung surface and microscopically on lung sections.

In a second experiment, 10^5 B16-F10 cells in 50 μ l PBS were injected IV into the lateral tail vein of C57BL/6J mice. They were then treated twice with adenovirus vector, once 2 days after B16-F10 injection and once 1 week later. Some of the mice ($n = 7$ /group) were killed 22 days after tumor cell injection and the remaining mice ($n = 4$ /group) were killed 5 days later.

Immunoprecipitation

Fifty microliters of serum collected from the lung metastasis experiment was added to 450 μ l PBS containing protease inhibitors (Complete Mini Protease Inhibitor Cocktail) (Roche, Mannheim, Germany). The different sera were then incubated with 50 μ l protein A agarose (Roche, Mannheim, Germany) for 1 hour at 4 °C under rotation. The solutions were centrifuged for 20 seconds at 6,000 rpm and 4 °C, then incubated on ice for 5 minutes. Ten microliters of rabbit polyclonal anti-16K hPRL antiserum (SB30) was added to each supernatant and the mix was incubated for 3 hours at 4 °C under rotation. Fifty microliters of protein A agarose was added to the mix and incubated overnight at 4 °C under rotation. After centrifugation for 20 seconds at 6,000 rpm and incubation on ice for 5 minutes, the supernatants were discarded and the pellets (containing the beads) were washed three times with PBS. After a new centrifugation, the beads were resuspended in 30 μ l $1 \times \beta$ -mercaptoethanol loading buffer and boiled at 100 °C for 5 minutes, then left on ice for 5 minutes. The beads were centrifuged for 5 minutes at 4 °C; then the supernatants were subjected to sodium dodecyl sulfate polyacrylamide gel electrophoresis (12% acrylamide) for Western blot analysis.

Western blot analysis

Proteins in 30 μ l immunoprecipitate or 30 μ l medium conditioned with COS cells infected at increasing an multiplicity of infection with 16K-Ad or Null-Ad were resolved by sodium dodecyl sulfate polyacrylamide gel electrophoresis and transferred to a polyvinylidene fluoride membrane (Millipore, Bedford, MA). Membranes were saturated for 1 hour in Tris-buffered saline-8% dry milk, followed by incubation for 1 hour with a 1/500 dilution of anti-16K hPRL antibody (SB30 for immunoprecipitates; A602 for conditioned media) and for 1 hour with a 1/5,000 dilution of peroxidase-conjugated goat antirabbit antibody (Gamma; BioWhittaker, Verviers, Belgium). 16K hPRL detection was carried out by chemiluminescence using the ECL Plus kit (Amersham Biosciences, Arlington Heights, IL).

Histology and immunohistochemistry

Tumors and lungs were either embedded in Tissue-Tek (Sakura Finetek, Zoeterwoude, The Netherlands) and frozen at -70 °C or fixed in 4% paraformaldehyde for 3-4 hours, dehydrated, and embedded in paraffin (Labonord, Templemars, France). The tissues were then sectioned (6 μ m thick). To study overall tissue morphology, slides of paraffin sections were soaked in XyloI (Sigma-Aldrich, Steinheim, Germany) to

deparaffinize them, then rehydrated in graded alcohol series (100-75%) and stained with hematoxylin/eosin. For assessment of angiogenesis, tumor, lung, and liver vessels were stained with CD31. For CD31 staining, frozen sections were fixed in 80% methanol (VWR, Leuven, Belgium) for 10 minutes at -20°C. Endogenous peroxidase was subsequently blocked with 3% H₂O₂/H₂O (Sigma-Aldrich, Steinheim, Germany) for 20 minutes, and non-specific binding was prevented in normal rabbit serum for 1 hour at RT. Sections were then incubated first with a rat monoclonal anti-CD31 (1/250; BD Biosciences, Erembodegem, Belgium) for 1 hour at RT, then with a biotinylated secondary antibody (1/400; DAKO, Heverlee, Belgium) for 30 minutes at RT. This was followed by incubation with streptavidin/horseradish peroxidase complex (1/500; DAKO, Heverlee, Belgium). CD31-positive cells were visualized after coloring sections for 3 minutes with 3-amino-9-ethylcarbazole (DAKO, Heverlee, Belgium). The sections were finally counterstained with hematoxylin and mounted for microscopy with Aqua Polymount (Polysciences, Warrington, PA).

Image processing and measurements

Images were digitized in $1,360 \times 1,024$ pixels in the red-green-blue color space. Image processing and measurements were performed with the software Aphelion 3.2 from Adsis (France) on a personal computer. Fifteen images, counting a total of ~500 vessels, were analyzed for each condition.

Immunostaining for CD31 of histological tumor sections is used to distinguish tumor vessels from tissue. They appear in red in the red-green-blue color image (Figure 4b, A). The red component of the red-green-blue color image was first extracted and the resulting image (Figure 4b, B) was further processed as follows: (i) tumor vessels were segmented automatically using the entropy of the histogram of gray-level intensities³⁰; (ii) an erosion morphological filter was applied to eliminate small artifacts; (iii) as this last operation reduces the size of vessels, a geodesic dilation was carried out to make them recover their real sizes; (iv) all vessels touching the border of the image were eliminated (Figure 4b, C); (v) in order to identify and measure the area of each vessel, the vessels were labeled with different colors (Figure 4b, D).

The following measurements were performed:

- (i) Vessel density defined as the number of vessels per unit of tissue area.
- (ii) Area density defined as the percentage of tissue area occupied by vessels.
- (iii) Vessel size distribution.

Statistical analysis

All data are expressed as means \pm SE. Analyses for statistical significance (the Mann-Whitney test) were carried out with Prism 4.0 software (GraphPad Software, San Diego, CA). Statistical significance was set at $P < 0.05$.

ACKNOWLEDGMENTS

The authors gratefully acknowledge the excellent technical assistance of Michelle Lion (Laboratory of Molecular Biology and Genetic Engineering) for Western blotting, Luc Duwez (Central Animal Facility of Centre Hospitalier Universitaire de Liège) for injecting animals IV and Isabelle Dasoul (Laboratory of Tumor and Development Biology) for immunohistochemical staining and advice. This work was supported by grants from the Fonds pour la Recherche industrielle et agricole and Télévie (to N.-Q.-N.N. and S.P.T.) and from the Fonds national pour la Recherche scientifique, the Belgian Federation against Cancer (a non-profit organization) and the Région Wallonne.

REFERENCES

1. Steeg, PS (2006). Tumor metastasis: mechanistic insights and clinical challenges, *Nat Med* 12: 895-904.
2. Fidler, IJ (2002). Critical determinants of metastasis. *Semin Cancer Biol* 12: 89-96,
3. Carmeliet, P (2005). Angiogenesis in life, disease and medicine. *Nature* 438: 932-936.
4. Zetter, BR (1998). Angiogenesis and tumor metastasis. *Annu Rev Med* 49: 407-424.
5. Ferrara, N and Kerbel, RS (2005). Angiogenesis as a therapeutic target. *Nature* 438: 967-974.

6. D'Angelo, G, Struman, I, Martial, JA and Weiner, RI (1995). Activation of mitogen-activated protein kinases by vascular endothelial growth factor and basic fibroblast growth factor in capillary endothelial cells is inhibited by the antiangiogenic factor 1 6-kDa N-terminal fragment of prolactin, *Proc Natl Acad Sci USA* 92: 6374-6378.
7. D'Angelo, G, Martini, JF, Iri, T, Fantl, WJ, Martial, JA and Weiner, RI (1999). 16K human prolactin inhibits vascular endothelial growth factor-induced activation of Ras in capillary endothelial cells. *Mol Endocrinol* 13: 692-704.
8. Lee, H, Struman, I, Clapp, C, Martial, JA and Weiner, RI (1998). Inhibition of urokinase activity by the antiangiogenic factor 1 6K prolactin: activation of plasminogen activator inhibitor 1 expression. *Endocrinology* 139: 3696-3703.
9. Martini, JF, Piot, C, Humeau, LM, Struman, I, Martial, JA and Weiner, RI (2000). The antiangiogenic factor 16K PRL induces programmed cell death in endothelial cells by caspase activation. *Mol Endocrinol* 14: 1536-1549.
10. Tabruyn, SP, Sorlet, CM, Rentier-Delrue, F, Bours, V, Weiner, RI, Martial, JA *et al.* (2003). The antiangiogenic factor 1 6K human prolactin induces caspase-dependent apoptosis by a mechanism that requires activation of nuclear factor- κ B. *Mol Endocrinol* 17: 1815-1823.
11. Tabruyn, SP, Nguyen, NQ, Comet, AM, Martial, JA and Struman, I (2005). The antiangiogenic factor, 16-kDa human prolactin, induces endothelial cell cycle arrest by acting at both the G0-G1 and the G2-M phases. *Mol Endocrinol* 19: 1932-1942.
12. Hilfiker-Kleiner, D, Kaminski, K, Podewski, E, Bonda, T, Schaefer, A, Sliwa, K *et al.* (2007). A cathepsin D-cleaved 1 6kDa form of prolactin mediates postpartum cardiomyopathy. *Cell* 128: 589-600.
13. Bentzien, F, Struman, I, Martini, JF, Martial, JA and Weiner, RI (2001). Expression of the antiangiogenic factor 1 6K hPRL in human HCT116 colon cancer cells inhibits tumor growth in Rag1^{-/-} mice. *Cancer Res* 61: 7356-7362.
14. Kim, J, Luo, W, Chen, DT, Earley, K, Tunstead, J, Yu-Lee, LY *et al.* (2003). Antitumor activity of the 1 6-kDa prolactin fragment in prostate cancer. *Cancer Res* 63: 386-393.
15. Pan, H, Nguyen, NQ, Yoshida, H, Bentzien, F, Shaw, LC, Rentier-Delrue, F *et al.* (2004). Molecular targeting of antiangiogenic factor 1 6K hPRL inhibits oxygen-induced retinopathy in mice. *Invest Ophthalmol Vis Sci* 45: 2413-2419.
16. Cao, Y (2001). Endogenous angiogenesis inhibitors and their therapeutic implications, *Int J Biochem Cell Biol* 33: 357-369.
17. Dkhissi, F, Lu, H, Soria, C, Opolon, P, Griscelli, F, Liu, H *et al.* (2003). Endostatin exhibits a direct antitumor effect in addition to its antiangiogenic activity in colon cancer cells. *Hum Gene Ther* 14: 997-1008.
18. Hajitou, A, Sounni, NE, Devy, L, Grignet-Debrus, C, Lewalle, JM, Li, H *et al.* (2001). Down-regulation of vascular endothelial growth factor by tissue inhibitor of metalloproteinase-2: effect on *in vivo* mammary tumor growth and angiogenesis. *Cancer Res* 61: 3450-3457.
19. Streit, M, Riccardi, L, Velasco, P, Brown, LF, Hawighorst, T, Bornstein, P *et al.* (1999). Thrombospondin-2: a potent endogenous inhibitor of tumor growth and angiogenesis. *Proc Natl Acad Sci USA* 96: 14888-14893.
20. Blazquez, C, Casanova, ML, Planas, A, Del Pulgar, TG, Villanueva, C, Fernandez-Acenero, MJ *et al.* (2003). Inhibition of tumor angiogenesis by cannabinoids. *FASEB J* 17: 529-531.
21. Gonzalez, C, Corbacho, AM, Eiserich, JP, Garcia, C, Lopez-Barrera, F, Morales-Tlalpan, V *et al.* (2004). 1 6K-prolactin inhibits activation of endothelial nitric oxide synthase, intracellular calcium mobilization, and endothelium-dependent vasorelaxation. *Endocrinology* 145: 5714-5722.
22. Woodhouse, EC, Chuaqui, RF and Liotta, LA (1997). General mechanisms of metastasis. *Cancer* 80(8 suppl.): 1529-1537.
23. Sauter, BV, Martinet, O, Zhang, WJ, Mandeli, J and Woo, SL (2000). Adenovirus-mediated gene transfer of endostatin *in vivo* results in high level of transgene expression and inhibition of tumor growth and metastases. *Proc Natl Acad Sci USA* 97: 4802-4807.
24. Lalani, AS, Chang, B, Lin, J, Case, SS, Luan, B, Wu-Prior, WW *et al.* (2004). Anti-tumor efficacy of human angiostatin using liver-mediated adeno-associated virus gene therapy. *Mol Ther* 9: 56-66.
25. Mah-Becherel, MC, Ceraline, J, Deplanque, G, Chenard, MP, Bergerat, JP, Cazenave, JP *et al.* (2002). Anti-angiogenic effects of the thienopyridine SR 25989 *in vitro* and *in vivo* in a murine pulmonary metastasis model. *Br J Cancer* 86: 803-810.
26. Niu, G, Xiong, Z, Cheng, Z, Cai, W, Gambhir, SS, Xing, L *et al.* (2007). *In vivo* bioluminescence tumor imaging of RGD peptide-modified adenoviral vector encoding firefly luciferase reporter gene. *Mol Imaging Biol* 9:126-134.
27. Liu, Y, Koziol, J, Deisseroth, A and Borgstrom, P (2007). Methods for delivery of adenoviral vectors to tumor vasculature. *Hum Gene Ther* 18: 151-160.
28. Paris, N, Rentier-Delrue, F, Defontaine, A, Goffin, V, Lebrun, JJ, Mercier, L *et al.* (1990). Bacterial production and purification of recombinant human prolactin, *Biotechnol Appl Biochem* 12: 436-449.

29. Sun, J, Blaskovich, MA, Jain, RK, Delarue, F, Paris, D, Brem, S *et ai.* (2004), Blocking angiogenesis and tumorigenesis with GFA-11 6, a synthetic molecule that inhibits binding of vascular endothelial growth factor to its receptor. *Cancer Res* 64: 3586-3592.
30. Sahoo, PK, Soltani, S, Wong, AKC and Chen, YC (1 988). A survey of thresholding techniques. *Comp Vis Graph Image Proc* 41: 223-260,